Excitons and Resonant Inelastic X-Ray Scattering in Graphite

Michel van Veenendaal and Paolo Carra

European Synchrotron Radiation Facility, B.P. 220, F-38043 Grenoble Cédex, France
(Received 26 November 1996)

X-ray resonant inelastic scattering in graphite is analyzed including the effect of a screened core-hole Coulomb potential in the intermediate state. Numerical calculations of the scattered intensity are reported. Evidence for the presence of excitonic states in the observed K-edge spectra is provided, thus identifying a major drawback in the use of resonant scattering as a probe of electronic band structures. [S0031-9007(97)02852-4]

The high brilliance of synchrotron radiation sources has stimulated a number of experimental investigations as to the applicability of resonant inelastic x-ray scattering (RIXS) to determine the electronic structure of solids. The probe detects electronic excitations of energy $\omega = \omega_1 - \omega_2$ and momentum $\mathbf{q} = \mathbf{q}_1 - \mathbf{q}_2$, as allowed by the corresponding conservation laws. (The subscripts denote ingoing and outgoing photons; $\hbar = 1$.) The physical information these experiments provide is recorded as a function of ω_1 and ω_2, at a given $\mathbf{q}$; usually, the emission spectrum is analyzed for a discrete set of ω_1 values, which are taken across an absorption threshold [1–6]. Compared to photoelectron spectroscopy, the technique has the advantage of a negligible surface sensitivity and of being free from charging effects; given its element specificity, it could provide a useful alternative to photoemission in multielement materials.

Localized electronic states have been probed with RIXS, as have broad bands. Spectra, observed in $3d$ transition metals and rare earths, have been explained within atomic theory, calculating the permitted decays from the intermediate-state multiplets [7,8]. Such a description is inappropriate to discuss the data collected from diamond [1,2], B_2O_3 [3], boron nitride [3,6], silicon [4], and graphite [5]. An interpretation of the emission profiles has been put forward in the framework of one-electron (independent quasiparticle) theory [2], for these systems.

RIXS is accurately accounted for by the lowest Born approximation. In the one-electron limit the final state of the target differs from the initial one by the presence of one electron-hole pair in the conduction-valence bands; the double-differential scattering cross section reflects the joint density of states, weighed by the oscillator strength of the local core-level transitions. Moreover, in certain electronic structures, the crystal momentum of the excited electron is (almost) uniquely determined at a given absorption energy; an ω_2 scan maps the momentum-resolved structure of the valence band, in these cases.

As reported by Carlisle and collaborators [5], the observation of dispersive features about the K edge of graphite ($\simeq$284 eV) has been interpreted as providing

strong support to the validity of the foregoing picture, which neglects the Coulomb interaction between the deep $1s$ hole and the promoted electron. (For convenience of the reader, the data of Ref. [5] are reproduced in Fig. 1.) It is important to notice that numerical calculations, based on *ab initio* graphite band structures, do not correctly reproduce the near-edge emission profiles of Fig. 1. A satisfactory agreement is obtained when a fraction of the $\omega_1 = 400$ eV spectrum is included, thus introducing a somewhat arbitrary superposition of events which are far removed in energy [5]; conceptually, this procedure
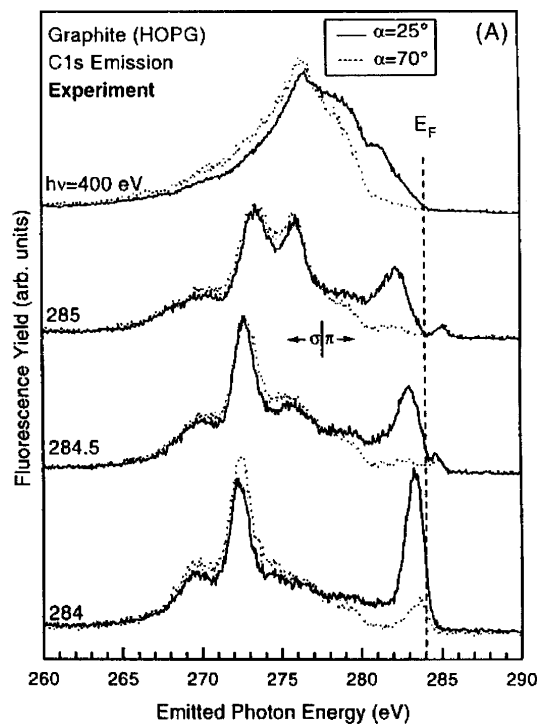

FIG. 1. Graphite RIXS spectra obtained by Carlisle and co-workers, for two different photon takeoff angles: $\alpha = 25°$ (solid lines) and $\alpha = 70°$ (dotted lines). Experimental geometry: The scattering plane is perpendicular to the graphite planes; the ingoing photon is linearly polarized in the scattering plane, and the outgoing polarization is not detected. The scattering angle is fixed at 90°. (Reproduced from Ref. [5].)

implies an ill-defined distinction between coherent and incoherent scattering processes [9].

Objections to the applicability of one-electron theory to describe the graphite data have been raised by Brühwiler and co-workers [10]. These authors have stressed the possible importance of excitonic and vibronic effects in the intermediate state.

This Letter reports numerical results for the RIXS cross section at the carbon K edge in graphite; excitonic effects are included by considering an intermediate-state Coulomb potential, which acts between the 1s hole and band electrons. The calculated emission spectra are in satisfactory agreement with the experimental observations.

Theoretical framework.—We consider the resonant transition amplitude (at $T = 0$, and assuming $E_i = 0$),

$$U_{i \rightarrow f} = \langle f | H_{\text{int}} G(\omega_1) H_{\text{int}} | i \rangle ,$$

as determined by the coupling of the photon to the electron paramagnetic current

$$H_{\text{int}} = -\frac{e}{mc} \int d\mathbf{r} \mathbf{A}(\mathbf{r}) \cdot \Psi^{\dagger}(\mathbf{r}) \mathbf{p} \Psi(\mathbf{r}) . \quad (1)$$

The intermediate-state propagator is defined by

$$G(\omega) = \lim_{\eta \rightarrow 0} (\omega - H + i\eta)^{-1} ,$$

with H the electron Hamiltonian. The total scattering rate (golden rule) reads

$$P_{\text{tot}}(\omega_1, \omega_2) = \frac{2\pi}{\hbar} \sum_f |U_{i \rightarrow f}|^2 \delta(E_f + \omega_2 - \omega_1) .$$

A simple expression for the electron field operator, which appears in Eq. (1), is provided by

$$\Psi(\mathbf{r}) = \sum_{\mathbf{k}}^{BZ} \sum_{\mu} a_{\mu,\mathbf{k}} \psi_{\mu,\mathbf{k}}(\mathbf{r}) + \sum_{\mathbf{k}}^{BZ} \sum_{\mu} b_{\mu,\mathbf{k}}^{\dagger} \psi_{\mu,\mathbf{k}}(\mathbf{r}) .$$

The notation is as follows. We adopt the particle-hole picture: Electron annihilation and hole creation operators are denoted by $a_{\mu,\mathbf{k}}$ and $b_{\mu,\mathbf{k}}^{\dagger}$, respectively. (Summations run over occupied and unoccupied levels, accordingly.)

Band electrons are identified by a band index and spin $\mu = n\sigma$; core states are labeled by atomic quantum numbers $\mu = jm$, with $j = c \pm \frac{1}{2}$; $\psi_{\mathbf{k}}(\mathbf{r})$ represents a Bloch electron.

Expanding the vector potential in plane waves, the transition amplitude can be given the form

$$U_{i \rightarrow f} = \mathcal{N} \sum_{\mathbf{k}\mathbf{k'}}^{BZ} \sum_{jm,j'm'} \sum_{\mu,\mu'} M_{\mu,jm}(\mathbf{k} + \mathbf{q}_1, \boldsymbol{\epsilon}_1)$$
$$\times M_{\mu',jm'}^{*}(\mathbf{k'} + \mathbf{q}_2, \boldsymbol{\epsilon}) \langle f | b_{jm',\mathbf{k'}} b_{\mu',\mathbf{k'}+\mathbf{q}_2}^{\dagger}$$
$$\times G(\omega_1) a_{\mu,\mathbf{k}+\mathbf{q}_1}^{\dagger} b_{jm,\mathbf{k}}^{\dagger} | i \rangle , \quad (2)$$

where $\mathcal{N} = 2\pi e^2/(m^2 V \sqrt{\omega_1 \omega_2})$, with V a quantization volume; $\boldsymbol{\epsilon}_1$ and $\boldsymbol{\epsilon}_2$ denote photon polarizations. (Reciprocal lattice vectors have been omitted.) For electric-dipole transitions, the one-electron matrix element is defined by

$$M_{\mu,jm}(\mathbf{k}, \boldsymbol{\epsilon}) = \sum_{\mathbf{R}} e^{-i\mathbf{k} \cdot \mathbf{R}} \boldsymbol{\epsilon} \cdot \int d\mathbf{r} \varphi_{\mu}^{*}(\mathbf{r} - \mathbf{R}) \, \mathbf{p} \, \varphi_{jm}(\mathbf{r}) ,$$

with $\mathbf{R}$ a site label in a lattice of N sites; φ denotes a Wannier's function. A symmetry analysis serves to identify charge and magnetic contributions to $U_{i \rightarrow f}$ [11–13]; our considerations will be restricted to pure charge scattering.

Electronic relaxation in the resonant process is studied by considering an electron Hamiltonian of the form $H = H_0 + H_1$, with H_0 describing motion in a periodic structure, and

$$H_1 = \frac{1}{2} \sum_{\mathbf{k},\mathbf{k'},\mathbf{q}} \sum_{\text{all} \mu,j,m} V_{\mu',j'm';\mu,jm}(\mathbf{q})$$
$$\times a_{\mu'\mathbf{k'}+\mathbf{q}}^{\dagger} b_{jm\mathbf{k}-\mathbf{q}} b_{j'm'\mathbf{k}}^{\dagger} a_{\mu\mathbf{k'}} \quad (3)$$

accounting for the presence of a core-hole Coulomb potential in the intermediate state. (The rigid shift of a fully occupied band has not been included in H_1.) As usual, $G = G_0 + G_0 H_1 G$, defining the particle-hole Green function. In the many-electron Bloch representation, free-intermediate-state propagation is described by

$$\langle \mu_4, \mathbf{k}_4; \underline{jm_3, \mathbf{k}_3} | G_0(\omega) | \mu_2 \mathbf{k}_2; \underline{jm_1 \mathbf{k}_1} \rangle = \frac{\delta_{\mu_4 \mathbf{k}_4, \mu_2 \mathbf{k}_2} \delta_{m_3 \mathbf{k}_3, m_1 \mathbf{k}_1}}{\omega - \varepsilon_{\mu_2, \mathbf{k}_2} + \varepsilon_{jm_1, \mathbf{k}_1} + i\eta} , \quad (4)$$

with ε denoting one-electron energies. (Hole states are underlined.)

Scattering in the independent quasiparticle limit.—Inserting the free propagator $G_0(\omega_1)$ into expression (2), we obtain

$$U_{i \rightarrow f}^{0} = \mathcal{N} \sum_{\mathbf{k}}^{BZ} \sum_{\mu,\mu',jm} M_{\mu,jm}(\mathbf{k} + \mathbf{q}_1, \boldsymbol{\epsilon}_1) M_{\mu',jm}^{*}(\mathbf{k} + \mathbf{q}_2, \boldsymbol{\epsilon}_2)$$
$$\times \frac{\langle f | a_{\mu,\mathbf{k}+\mathbf{q}_1}^{\dagger} b_{\mu',\mathbf{k}+\mathbf{q}_2}^{\dagger} | i \rangle}{\omega_1 - \varepsilon_{\mu,\mathbf{k}+\mathbf{q}_1} + \varepsilon_{jm,\mathbf{k}} + i\eta} , \quad (5)$$

with $|f\rangle = |\tilde{\mu}, \tilde{\mathbf{k}} + \mathbf{q}_1; \underline{\tilde{\mu}', \tilde{\mathbf{k}} + \mathbf{q}_2} \rangle$ and $E_f = \varepsilon_{\tilde{\mu}, \tilde{\mathbf{k}}+\mathbf{q}_1} - \varepsilon_{\tilde{\mu}', \tilde{\mathbf{k}}+\mathbf{q}_2}$.

Expression (5) yields the scattering amplitude in the independent quasiparticle limit. When such an approximation holds, the scattering rate $P_{\text{tot}}^{0}(\omega_1, \omega_2)$ provides a mapping of the joint density of states of the system. Various features of this three-dimensional structure could then be probed using different experimental setups. A specific example: Keeping ω_1 fixed, while varying ω_2, amounts to moving through the valence-band structure. All accessible crystal momenta $\mathbf{k}$ will be superimposed at a given energy ω_1 and the momentum resolution of the mapping blurred, in the general case. Notice that different values of $\mathbf{k}$ add up incoherently; in fact, using $\sum_f \rightarrow \sum_{\tilde{\mu}, \tilde{\mu}', \tilde{\mathbf{k}}}$ it

is straightforward to prove that $P_{\text{tot}}^0(i \to f) \sim N$, indicating a *spatially incoherent process*. $P_{\text{tot}}^0(i \to i) \sim N^2$, so that coherence is recovered in the elastic limit. (To higher order in G, interference terms appear; still, inelastic scattering remains incoherent as one expects.)

To compare the graphite data of Fig. 1 with the predictions of one-electron theory, we have performed numerical calculations of $P_{\text{tot}}^0(\omega_1, \omega_2)$, for $\omega_1 = 0, 0.5, 1.0$, and 1.5 eV. (Photon energies are measured from the absorption threshold.) In the numerical work, the Wannier functions of our general formalism have been replaced with a basis set of atomic orbitals $\psi_{\mu\mathbf{k}}(\mathbf{r}) = \sum_\lambda a_{\lambda\mu\mathbf{k}}\langle\mathbf{r}|\lambda\mathbf{k}\rangle$, with $\lambda \to \mathbf{R}_i, l, l_z, \sigma$; $\mathbf{R}_i$ runs over the atoms in a unit cell (lattice with a basis). Only vertical $M_{n,1s}(\mathbf{k}, \boldsymbol{\epsilon})$ transitions have been considered, thus disregarding the effects of a small but finite (about one tenth of the Brillouin zone) photon wave vector. The spin dependence (diagonal) has been neglected. We assumed a core-hole width $\Gamma_{1s} = 0.075$ eV (FWHM); experimental resolution was accounted for by convoluting the spectra with a $\sigma = 0.5$ eV Gaussian line shape.

The results are plotted in Fig. 2 (lower panel, dashed lines); they have been obtained from the graphite band structure depicted in Fig. 2 (upper panel), which we determined by implementing the Slater-Koster tight-binding parametrization scheme [14]. These emission spectra reflect a $1s \to \pi^*$ absorption process, near the K symmetry point, followed by emission from the π and σ bands at about 0, –11, and –14 eV. The changes in the spectral profiles, as ω_1 is swept from threshold to 1.5 eV above, are readily explained by following the band structure in the $K \to \Gamma$ direction.

Notice that *one-electron theory provides no explanation for the emission peak observed at –8 eV*. As shown below, this discrepancy can be overcome by invoking intermediate-state relaxation.

Electronic relaxation.—The screening of a carbon $1s$ hole in graphite (a semimetal) has been a point of discussion. The lack of agreement between the one-electron density of states and absorption spectra (electron-energy-loss data) was interpreted by Mele and Ritsko [15] as a clear indication of a strong excitonic shift in the final state. Their findings were contradicted by Weng *et al.* [16], and by Batson [17]; these authors claimed that a minor (virtually negligible) excitonic enhancement was sufficient for
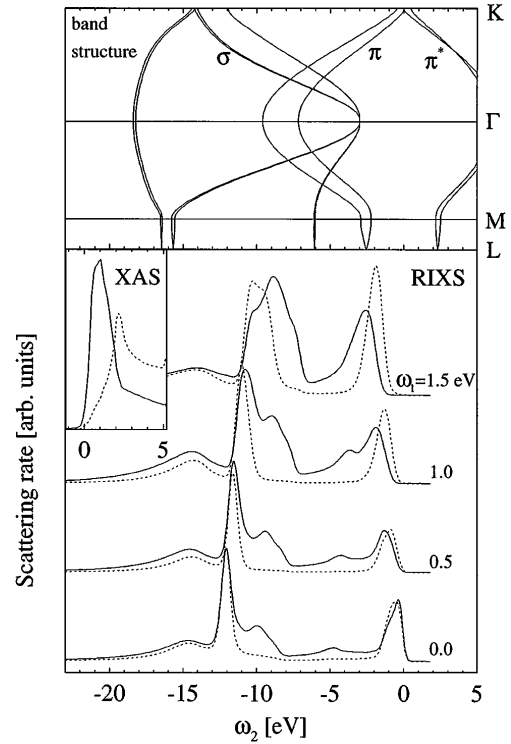

FIG. 2. Upper panel: the band structure of graphite. Lower panel: numerical calculations of the graphite K-edge emission spectra for $\alpha = 25°$, in the scattering geometry of Fig. 1. The independent quasiparticle approximation is given by the dashed lines. The inclusion of a local $U = -3$ eV core-hole potential is represented by the solid lines. The corresponding absorption (XAS) profiles are depicted in the inset.

modeling the measured K-shell near-edge structure. More recently, core-hole autoionization spectroscopy has provided further support to the view that, near threshold, the excited electron is localized [18,19]; thus, excitons significantly contribute to electronic screening.

In the presence of intermediate-state relaxation the scattering amplitude is governed by the particle-hole propagator G, and numerical calculations of the spectra have been performed by proceeding as follows. We assumed a local potential and set $(1/2)V_{\mu'\frac{1}{2}\sigma;\mu,\frac{1}{2}\sigma'}(\mathbf{q}) = \sum_\lambda U(\lambda)\langle\lambda\mathbf{k}'|\mu'\mathbf{k}'\rangle\langle\lambda\mathbf{k}|\mu\mathbf{k}\rangle\delta_{\sigma,\sigma'}$ in the definition of H_1; electron-hole pair creation has been neglected. In this case relaxation reduces to an exactly solvable, two-particle problem; the propagator reads

$$\langle\mu'\mathbf{k}'; 1s\mathbf{k}'|G(\omega_1)|\mu\mathbf{k}; 1s\mathbf{k}\rangle = G_0^{\mu\mathbf{k}}(\omega_1)\delta_{\mu,\mu'}\delta_{\mathbf{k}',\mathbf{k}} + \frac{G_0^{\mu\mathbf{k}}(\omega_1)\sum_\lambda\langle\mu\mathbf{k}|\lambda\mathbf{k}\rangle U\langle\lambda\mathbf{k}'|\mu'\mathbf{k}'\rangle G_0^{\mu'\mathbf{k}'}(\omega_1)}{1 - U\sum_{\lambda\mu\mathbf{k}} G_0^{\mu\mathbf{k}}(\omega_1)|\langle\lambda\mathbf{k}|\mu\mathbf{k}\rangle|^2},$$

with $G_0^{\mu\mathbf{k}}(\omega_1) = (\omega_1 - \varepsilon_{\mu\mathbf{k}} + \varepsilon_{1s\mathbf{k}} + i\frac{\Gamma_{1s}}{2})^{-1}$ and $\langle\lambda\mathbf{k}|\mu\mathbf{k}\rangle = a_{\lambda\mu\mathbf{k}}$. (The potential strength U is in general λ dependent; however, the graphite near-edge structure is entirely determined by p_z orbitals, and this dependence can be omitted.) The relevant effect of G (central-cell

exciton) is pictured in Fig. 3. The calculated scattering rates $P_{\text{tot}}(\omega_1, \omega_2)$ are depicted in Fig. 2 (lower panel, solid lines). U is a free parameter in our model; to obtain an absorption-peak shift close to the observed value, we have set $U = -3$ eV, in agreement with Ref. [15]. Our
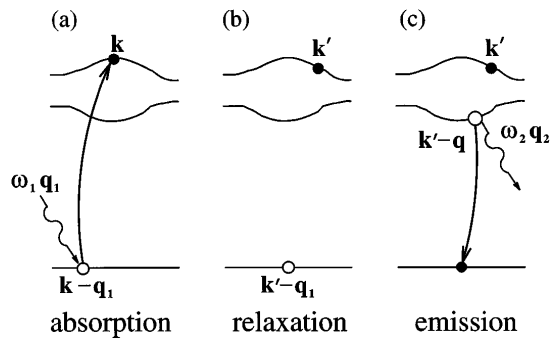
FIG. 3. Schematic representation of intermediate-state relaxation. (a) Absorption of a photon $\mathbf{q}_1$, ω_1 through the excitation of a core electron into the conduction band. (b) $\mathbf{k} \rightarrow \mathbf{k}'$ propagation of the electron-core-hole pair. (c) Radiative decay of the intermediate state by creation of a valence-band hole with momentum $\mathbf{k}' - \mathbf{q}$ and emission of a photon $\mathbf{q}_2$, ω_2. ($\mathbf{k}' = \mathbf{k}$ in the independent quasiparticle limit.)

calculated absorption coefficients are shown in the inset of Fig. 2.

Going back to the RIXS spectra, we notice that an excitonic peak has appeared at about -8.5 eV in the numerical calculations; it is mainly a result of dipole transitions into the flat-band region between the L and M symmetry points. M is a saddle point in the π^* band and gives rise to the singularity in the graphite density of states. (See the inset in Fig. 2, dashed line [20].) These states are pulled down by the core-hole Coulomb interaction; consequently, the absorption process is allowed closer to threshold. [Notice that, in the presence of relaxation, $\omega_2 = \omega_1 - (\varepsilon_{\mu,\mathbf{k}'+\mathbf{q}_1} - \varepsilon_{\mu',\mathbf{k}'+\mathbf{q}_2})$, with $\omega_1 \neq \varepsilon_{\mu,\mathbf{k}'+\mathbf{q}_1} - \varepsilon_{jm,\mathbf{k}'}$, and emission from the central region of the Brillouin zone is negligible. As a result the angular dependence of the spectra is rather simple: a scaling of the π-band emission (from 0 to -6 eV) relative to the σ one (≤ -6 eV), in agreement with the experiment.]

In summary, this work has discussed general features of x-ray resonant inelastic scattering in solids. Numerical calculations of the total scattering rate at the carbon K edge in graphite have also been presented and compared with recent experiments. It has been shown that, in the independent quasiparticle limit (Bloch electrons) the process is incoherent, the underlying (theoretical) band structure being reflected in the spectra regardless. This description fails to reproduce the experimental data for two reasons: first, the calculated dispersion of the peaks attributed to the band structure is much smaller than the measured one; and second, important experimental features are not reproduced. To remove this discrepancy, we have included intermediate-state relaxation, in the form of excitonic states determined by the core-hole Coulomb potential; the resulting numerical graphite spectra are now in satisfactory agreement with the observations. (These excitonic effects should also be present in diamond, silicon, boron nitride, and B_2O_3.)

[1] J.-E. Rubensson, D. Mueller, R. Shuker, D. L. Ederer, C. H. Zhang, J. Jia, and T. A. Calcott, Phys. Rev. Lett. **64**, 1047 (1990).

[2] Y. Ma, N. Wassdahl, P. Skytt, J. Guo, J. Nordgren, P. D. Johnson, J.-E. Rubensson, T. Boske, W. Eberhardt, and S. Kevan, Phys. Rev. Lett. **69**, 2598 (1992).

[3] W. L. O'Brien, J. Jia, Q-Y. Dong, T. A. Calcott, K. E. Miyano, D. L. Ederer, D. R. Mueller, and C-C. Kao, Phys. Rev. Lett. **70**, 238 (1993).

[4] Y. Ma, K. E. Miyano, P. L. Cowan, Y. Aglitzkiy, and B. A. Karlin, Phys. Rev. Lett. **74**, 478 (1995).

[5] J. A. Carlisle, E. L. Shirley, E. A. Hudson, L. J. Terminello, T. A. Calcott, J. J. Jia, D. L. Ederer, R. C. C. Perera, and F. J. Himpsel, Phys. Rev. Lett. **74**, 1234 (1995).

[6] J. J. Jia, T. A. Calcott, E. L. Shirley, J. A. Carlisle, L. J. Terminello, A. Asfaw, D. L. Ederer, F. J. Himpsel, and R. C. C. Perera, Phys. Rev. Lett. **76**, 4054 (1996).

[7] F. M. F. de Groot, M. A. Arrio, Ph. Sainctavit, Ch. Cartier, and C. T. Chen, Solid State Commun. **92**, 991 (1994).

[8] M. van Veenendaal, J. B. Goedkoop, and B. T. Thole, Phys. Rev. Lett. **77**, 1508 (1996).

[9] Y. Ma, Phys. Rev. B **49**, 5799 (1994).

[10] P. A. Brühwiler, P. Kuiper, O. Eriksson, R. Ahuja, and S. Svensson, Phys. Rev. Lett. **76**, 1761 (1996).

[11] J. Luo, G. T. Trammell, and J. P. Hannon, Phys. Rev. Lett. **71**, 287 (1993).

[12] P. Carra and B. T. Thole, Rev. Mod. Phys. **66**, 1509 (1994).

[13] P. Carra and M. Fabrizio, in *Core Level Spectroscopies for Magnetic Phenomena: Theory and Experiment,* edited by P. S. Bagus, G. Pacchioni, and F. Parmigiani (Plenum Press, New York, 1995), p. 203.

[14] We remind the reader that the π bands are derived from the carbon $2p_z$ electrons (perpendicular to the graphite planes); the σ bands stem from the $2s$ and the in-planar $2p$ orbitals.

[15] E. J. Mele and J. J. Ritsko, Phys. Rev. Lett. **43**, 68 (1979).

[16] X. Weng, P. Rez, and H. Ma, Phys. Rev. B **40**, 4175 (1989).

[17] P. E. Batson, Phys. Rev. B **48**, 2608 (1993).

[18] P. A. Brühwiler, A. J. Maxwell, C. Puglia, A. Nilsson, S. Andersson, and N. Mårtensson, Phys. Rev. Lett. **74**, 614 (1995).

[19] R. Ahuja, P. A. Brühwiler, J. M. Wills, B. Johansson, N. Mårtensson, and O. Eriksson, Phys. Rev. B **54**, 14 396 (1996).

[20] Dispersion of the π^* band depends on the method used to determine the electronic structure. Current calculations predict no significant absorption at the M point, for excitation energies ≤ 1.3 eV above threshold. As demonstrated in Ref. [19] (supercell geometry), the π^* absorption resonance in graphite results from a Frenkel exciton.